THE JOURNAL OF PHYSICAL CHEMISTRY C

Article

Cite This: J. Phys. Chem. C 2019, 123, 21639−21644

pubs.acs.org/JPCC

Thermo-Electro-Mechanics at Individual Particles in Complex Colloidal Systems

Pavana Siddhartha Kollipara,[†] Linhan Lin,*[,†,‡,§] and Yuebing Zheng*[,†,‡]

[†]Walker Department of Mechanical Engineering and [‡]Materials Science & Engineering Program, Texas Materials Institute, The University of Texas at Austin, Austin, Texas 78712, United States

[§]Department of Precision Instruments, Tsinghua University, Beijing 100084, People's Republic of China

Supporting Information

ABSTRACT: It has been well established that thermoelectric (TE) field can arise from different Soret coefficients of salt ions in aqueous solution under constant temperature gradient. Despite their high relevance to cellular biology and particle manipulations, understanding and controlling of TE field in complex colloidal systems that involve micro/nanoparticles, salt ions, and molecules have remained challenging. In such colloidal systems, challenge arises from the thermal interactions with charged micro/nanoparticles that distort the TE field around the particles. Herein, we provide a framework for TE field in colloidal suspensions with various ions and surfactants at the single-nanoparticle level. In particular, we reveal the spatial variation of TE field around a dielectric particle under temperature gradient to determine the thermoelectric trapping force on the particle. Our theoretical results on the trapping stiffness predicted from the TE force profile match well with the experimental optothermoelectric trapping stiffness of particles in the solutions where the temperature gradient was well controlled by a laser beam. With insights into the TE field and force in complex systems, our framework and methodology can be extended to engineer the TE field for versatile optothermoelectric manipulations of arbitrarily shaped particles with nonuniform surface morphology and to advance the scientific research in cellular biology.

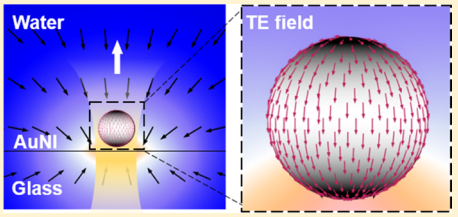

INTRODUCTION

Thermophoresis, also known as the Ludwig−Soret effect, is the response of molecules, ions, or micro/nanoparticles toward a thermal gradient. The thermophoresis-induced diffusion movement can be described by thermophoretic velocity $u_{th} = -D_T \nabla T$, where D_T is the thermal diffusion coefficient and ∇T is the externally imposed temperature gradient. In general, the sign of D_T is positive, indicating that molecules/colloids are thermophobic in nature.[1] Thermophilicity ($D_T < 0$) has also been observed in a few cases experimentally.[2] Because of their dependence on the inherent migration direction of the particles, applications based on thermophoresis are limited to colloidal particles with suitable compositions and migration direction. To tune the thermophoretic response of particles of expanded compositions, ionic compounds (salt or surfactant) are added to the solution to induce thermoelectric (TE) force for particle manipulations. Briefly, different Soret coefficients of individual charged ions in the solution lead to charge separation and result in a macroscopic TE field on the constituents of the system.[3] The direction of TE field can be reversed upon changing the constituent ions in the solution,[4] thereby controlling the migration direction of colloidal particles independent of the particle compositions. Applications exploiting this TE field have emerged in the fields of biology,[5,6] microparticle manipulation,[7,8] and microfluidic separation.[9] Moreover, electromagnetic waves have been used to generate optothermoelectric field through photon−phonon coupling to optically trap particles of various compositions and sizes.[10−13]

Quantification and control of TE field is crucial to all of the applications. Several theoretical studies were carried out to determine the TE field by analyzing the thermal diffusion coefficient or the Soret coefficient of micelles and charged colloids as a function of the nature of particle−solvent interface,[14] ionic strength,[15] colloid density,[16,17] and temperature.[18,19] Using such formulations, the thermophoretic velocity of a particle was evaluated by assuming a constant temperature gradient across the particle. The Navier−Stokes equations for the aqueous solution across constant temperature gradient have been solved to determine the volumetric force density on the solvent to evaluate TE force on the particle.[20,21] However, in real-life applications, temperature gradient across colloidal particles is achieved through external stimuli such as laser heating, where constant temperature gradient is invalid. In addition, large colloidal particles alter the temperature gradient around the particles due to difference in thermal conductivities of solute and solvent, which also contradicts the constant temperature gradient assumption. Therefore, to precisely determine the TE force on particles in complex colloidal systems, one needs a new methodology that considers

Received: July 6, 2019
Revised: August 4, 2019
Published: August 8, 2019

DOI: 10.1021/acs.jpcc.9b06425
J. Phys. Chem. C 2019, 123, 21639−21644

the temperature gradient change caused by the existence of the particles.

Here, we present a new thermo-electro-mechanical framework for TE force at dielectric microparticles that takes into account the particle-induced temperature gradient distortion. Using a commercial finite-element analysis (FEA) solver, we apply an externally imposed macroscopic temperature gradient field to a particle−surfactant solution. The resultant TE field due to the surfactant is evaluated using small-gradient approximation[22] and numerically integrated over the particle surface to obtain TE force. The significance of tangential and normal components of the TE field at the particle surface in controlling the particle motion is discussed. Subsequently, the theory is validated using experimentally measured trapping stiffness of polystyrene (PS) particles in cetyltetramethylammonium chloride (CTAC) solution under laser-heating-generated thermoelectric field (or optothermoelectric field).[23] We observe a good match between the theoretical trapping stiffnesses from the TE force profile of microparticles and the experimentally measured ones.

METHODS

Theory. Under steady conditions, the motion of an uncharged particle due to thermal gradient is balanced by the consequential concentration gradient achieved and is mathematically represented as

$$J_{\text{uncharged}} = 0 = -D\nabla \mathbf{c} - cD_{\text{T}}\nabla \mathbf{T} \tag{1}$$

where c is the concentration of the solute and D is the diffusion coefficient of the solute. Soret coefficient (S_{T}) is defined as the ratio D_{T}/D, which relates the concentration to temperature at steady state. In an electrolyte solution, molecules (i.e., salt and surfactant) dissociate into ions and each of the species moves differently under the thermal gradient due to dissimilar S_{T}, which results in an electric field. The ion flux under steady state is, therefore, a balance between concentration and thermal gradients along with the subsequent thermoelectric field and is represented as[19]

$$J_{\text{charged},i} = 0 = -D_i\nabla \mathbf{c_i} - c_iD_{\text{T},i}\nabla \mathbf{T} + \frac{Z_iec_i\mathbf{E_T}D_i}{k_{\text{B}}T} \tag{2}$$

where i represents index of ion, Z is the valency of ions, e is electron charge, E_{T} is the thermoelectric field generated, and k_{B} is the Boltzmann constant. The direction of TE field would be parallel or antiparallel to the temperature gradient depending on the charge of the species with the larger S_{T}[4] and is given as[18]

$$\mathbf{E_T} = \frac{k_{\text{B}}T\nabla \mathbf{T}}{e}\left(\frac{\sum X_ic_iS_{\text{Ti}}}{\sum X_i^2c_i}\right) \tag{3}$$

where $X_i = \pm 1$ for positive and negative ions, respectively. The net thermoelectric force F_{th} on a charged colloidal microparticle is then evaluated as qE_{T}, where q is the charge of the particle. However, eq 3 is valid only under the assumption that ∇T is uniform throughout the microparticle volume and that the net bulk charge density is zero. Figure 1a represents a system with an imposed uniform temperature gradient across the particle. Due to discontinuity in thermal conductivity at the particle−solvent interface, the temperature gradient deviates from the ideal constant temperature gradient in near-vicinity of the polystyrene (PS) particle, as shown in Figure 1b.

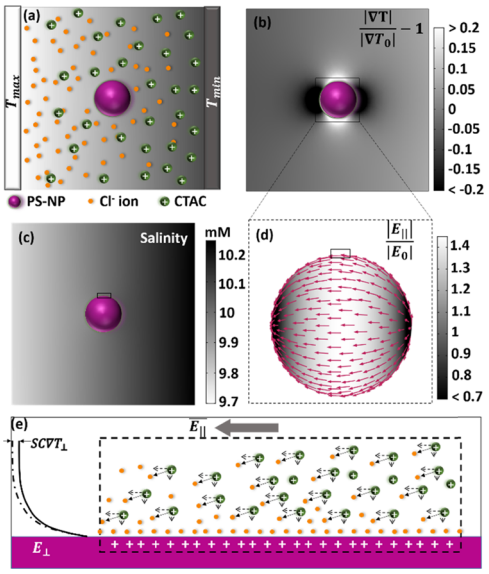

Figure 1. (a) Schematic of a constant temperature gradient system where the electrolyte ions diffuse at different rates. (b) Introduction of a particle in such a system distorts the uniform temperature gradient (∇T_0) around the particle surface. (c) Using small-gradient approximations, the salinity of the system for a temperature gradient of 20 K/μm is evaluated for 10 mM electrolyte solution. (d) Ratio of magnitude of $E_{\text{T},||}$ and E_0 (the bulk thermoelectric field due to a constant thermoelectric effect) shows that the effective tangential component is higher than that estimated at the surface. (e) Schematic for ion distributions around the particle surface. The chloride ions form a screening layer called Stern layer, and the free ions in the diffuse layer would be polarized while maintaining a near-zero charge density. Beyond the screening length (Debye length), $E_{\text{T},\perp}$ depends only on the temperature gradient (solid line) and tends to zero in the case of uniform temperature system (dot-dashed line).

Therefore, introduction of colloidal particles in a constant temperature gradient system inherently introduces a distortion in the temperature gradient, which necessitates the consideration of spatial varying temperature gradient and TE field to accurately determine TE force on the particles.

While TE field is being discussed, an important aspect to analyze is whether the temperature gradient is strong enough to overcome the electrostatic attractions, resulting in a macroscopic separation of ions. To understand such a separation, we need to know the salinity of the electrolyte solution. Salinity can be defined as the effective concentration of a charged electrolyte assuming that the bulk charge density due to ion dissociation is zero. In the current scenario, colloidal PS particles are dispersed in CTAC solution. The cation has a positive hydrophilic end and a hydrophobic polymer chain, enabling it to form micelles, which act as a macro-ion with a larger S_{T} due to the decreased diffusion coefficient (Supporting Information Note I). Owing to positive S_{T}, both micelles and chloride ions move toward the colder side, effectively lowering the "salinity" in the hot region. Figure 1c represents the salinity obtained as (Supporting Information Note II)

$$\frac{\nabla \mathbf{n_0}}{n_0} + \left(\frac{Z_2S_{\text{T}_1} - Z_1S_{\text{T}_2}}{Z_2 - Z_1}\right)\nabla \mathbf{T} = 0;\ n_0 = \frac{Z_1Z_2}{Z_1 - Z_2}(c_1 + c_2) \tag{4}$$

where salinity (n_0) is expressed as the combination of concentrations of ions such that net charge density is zero.

DOI: 10.1021/acs.jpcc.9b06425
J. Phys. Chem. C 2019, 123, 21639−21644

For a better estimate of TE field around the particle, individual concentrations of ions must be analyzed as deviations from the resultant salinity, as salinity acts a reference for zero ion dissociation. This can be obtained from Gauss law, where the net charge density at any position can be given as a function of TE field, $\rho/\epsilon = \nabla\cdot\mathbf{E}_T$, where ρ is the net charge density in a differential volume, given as $N_A e(Z_1c_1 + Z_2c_2)$, where N_A is the Avogadro number and ϵ is the permittivity of water as a function of temperature.[8] Using Gauss law along flux equations for micelles and counterions simultaneously, TE field can be determined around the particle. However, three-dimensional analysis of the system results in increased complications while solving coupled differential equations. To ease this numerical evaluation, small-gradient approximation is utilized, which leads to $\nabla\mathbf{n_0}/n_0 \sim \nabla\mathbf{c}_i/c_i \sim \nabla\mathbf{T}/T$ when $\delta T \ll T$.[22] This is a valid approximation as the maximum temperature difference considered in this work is 20 K, indicating that effective concentrations of ions can be approximated to salinity. Treating the micelle as a macro-ion, including the effects of accumulation number and effective charge on the micelle, we write the net thermoelectric field that is simplified as[22]

$$\mathbf{E_T} = \frac{k_B T\nabla\mathbf{T}}{e}\frac{\left[\frac{Z_1 S_{T_1}}{N_{agg}} + S_{T_2}\right]}{1 - \frac{Z_1 S_{T_1} T}{N_{agg}}} = \mathrm{SC}\nabla\boldsymbol{T} \tag{5}$$

where S_{T_1} and S_{T_2} are the Soret coefficients of the micelle[16] and chloride ion ($\sim 7.18 \times 10^{-4}$ K^{-1}),[24] respectively; N_{agg} is the number of ions forming a micelle aggregate ($\sim$89 for CTAC[25]); Z_1 is the effective charge on the micelle; and SC is the Seebeck coefficient. Equation 5 is only valid for a solution containing monovalent anion and macromicelle.

Although E_T is along the temperature gradient, the tangential and normal components of E_T at the particle surface have different effects on particle due to the electric charge on the particle. The tangential component $E_{T,\|}$ does not vanish at the surface and interacts with the particle's charge. Figure 1d shows that the magnitude of $E_{T,\|}$ has high deviations from TE field estimated using a constant temperature gradient ($|E_0| = |\mathrm{SC}\nabla T_0|$). The tangential component is numerically integrated around the surface to determine the effective TE force on the particle. On the other hand, the normal component of the thermoelectric field ($E_{T,\perp}$) is attenuated due to double-layer formation. The counterions in the solution are attracted to the charge of the particle and form an immovable layer known as "Stern layer" and a diffuse layer, which screens the remaining effect of the particle charge.[26] Figure 1e represents the Stern layer and diffuse region around the particle surface. The $E_\perp$ component is deviated by a magnitude of $\mathrm{SC}\nabla T_\perp$ in the bulk region in the presence of an external temperature gradient. The deviation minimizes while approaching the particle surface (Figure 1e, left). The net $E_\perp$ field at the particle surface is solely due to the charge on the particle, which does not influence motion of the particle.[27]

The effective TE force on the particle is subsequently evaluated by estimating the surface charge of the particle. A constant charge density can be assumed as charge redistribution does not occur under the influence of electric field on a dielectric particle.[27] The PS particles used are inherently negatively charged; however, due to CTAC adsorption on the particle, the net charge on the particle surface is positive, resulting in a positive ζ-potential.[23,28] The relation between the effective surface charge and the measured ζ-potential is given as[29]

$$\sigma = \frac{\epsilon\kappa k_B T}{e}\left[\exp\left(\frac{e\zeta}{2k_B T}\right) - \exp\left(-\frac{e\zeta}{2k_B T}\right) - \frac{4}{\kappa a}\frac{\left(\exp\left(\frac{e\zeta}{2k_B T}\right) - 1\right)}{\left(\exp\left(\frac{e\zeta}{2k_B T}\right) + 1\right)}\right] \tag{6}$$

where ζ is the measured ζ-potential and κ is the inverse Debye length and is dependent on the net concentration of the freely moving ions in the solution, given as

$$\kappa = \sqrt{\frac{e^2 N_A(2c_{cmc} + Q\times(c_0 - c_{cmc}))}{\epsilon k_B T}} \tag{7}$$

where c_{cmc} is the critical micellar concentration beyond which micelles are formed ($\sim$0.13 mM for CTAC) and N_A is the Avogadro number. The net TE force on the particle can be numerically integrated as

$$\mathrm{TE}_{force} = \int_A \sigma\mathbf{E}_{T,\|}\mathrm{d}A = \sum_{\theta=0}^{\pi}\sum_{\phi=0}^{2\pi}\sigma\mathbf{E}_{T,\|}a^2\sin(\theta)\,\mathrm{d}\theta\,\mathrm{d}\phi \tag{8}$$

Experiments. Our methodology can also be applied to colloidal systems with spatially varying temperature gradient field as long as the small-gradient approximation is valid. For experimental verification of our theory, optothermoelectric trapping (OTET) is employed to study the effects of thermoelectric force on PS particles in solution with CTAC surfactant. OTET uses laser heating of quasi-continuous gold nanoparticle substrate,[23] where photon−phonon conversion at the substrate and diffusion of temperature at the focal spot lead to a thermal gradient. Directed toward the center of the focal beam, the thermal gradient leads to the optothermoelectric field that enables trapping of the PS particles at the heating spot. For detailed experimental procedure and sample preparation, see Supporting Information Note IV. Along with TE force, optical and osmotic forces on the particle are also considered (Supporting Information Note V). We limit this work to in-plane trapping stiffness evaluation using TE field, and additional forces like depletion, van der Waals, and electrostatic repulsion act in the evaluation of z-directional trapping stiffness.

Figure 2a describes the computational geometry of the colloidal system under a laser-beam-generated thermal gradient. The gold nanoparticle substrate is at the interface of water and glass, and the heat retained within the substrate is negligible. The absorbed power by water is modeled as a Gaussian heat influx at the interface of glass and water. The simulation volume is large enough to assume a constant temperature as boundary conditions for glass and water media. Inside the water medium, a PS particle is introduced to account for the distortion of temperature gradient around the particle. The effective temperature gradient and the parallel component of the thermoelectric field are evaluated on the PS surface and numerically integrated to evaluate the TE force on the particle using eq 8. This simulation is repeated for several

DOI: 10.1021/acs.jpcc.9b06425
J. Phys. Chem. C 2019, 123, 21639−21644

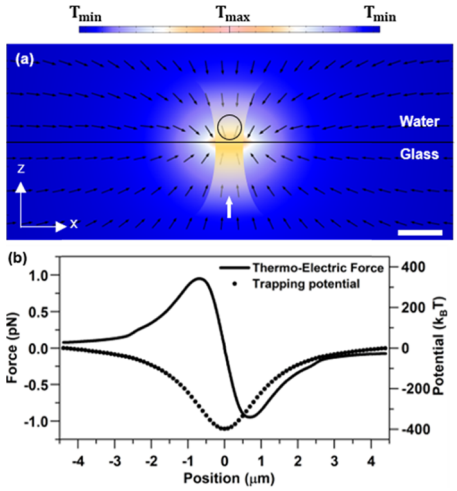

Figure 2. (a) Schematic for optothermoelectric trapping of a single PS particle. The arrow direction indicates the thermal gradient towards the hotspot. The scale bar is 1 μm. (b) The TE force on PS surface is evaluated as a function of position of particle using eq 8. The TE force along with optical and osmotic forces constitutes a trapping well of depth ~400 k_BT for a low laser power of ~135 μW.

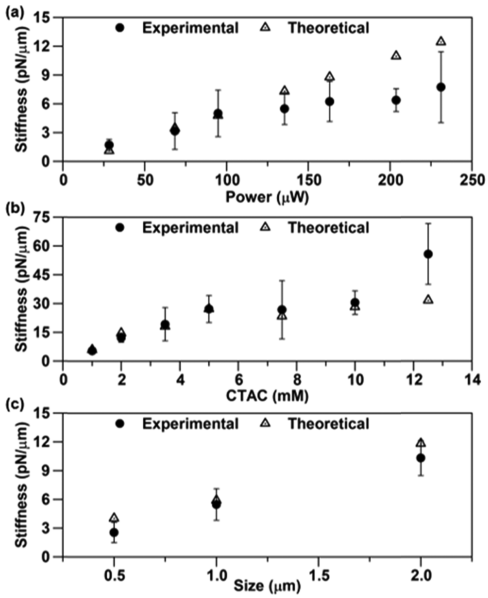

Figure 3. Experimental and theoretical values of trapping stiffnesses of polystyrene particles dispersed in CTAC solution as a function of (a) laser power (CTAC 1 mM and PS 1 μm), (b) CTAC concentration (power 135 μW and PS 1 μm), and (c) size of PS (power 135 μW and CTAC 1 mM).

positions of the particle along the substrate, and TE force is represented as a function of position in Figure 2b. For a comprehensive account of FEA simulations, see Supporting Information Note VI.

The net force $F = F_{TE} + F_{optical} + F_{osmotic}$ is used to evaluate the in-plane trapping potential as $U = -\int F\,dx$, although F_{TE} is higher by 2 orders of magnitude than $F_{optical}$ and $F_{osmotic}$. Figure 2b shows that, for a low laser power of ~135 μW, the theoretically obtained in-plane trapping potential is roughly 400 k_BT for a PS particle of 1 μm in diameter. For a similar laser power, the net trapping force is 2−3 orders higher in magnitude than that of optical tweezers.[30] Due to thermal diffusion of heat generated at the interface, the observed particle trapping is a long-range phenomenon. The force on the particle follows Hooke's law around the beam center, where trapping stiffness k_x is defined as $-\partial F/\partial x$ at the beam center.

RESULTS AND DISCUSSION

Laser Power. Figure 3a shows the variation of trapping stiffness of 1 μm PS particle with respect to the laser power at a constant CTAC concentration of 1 mM. Increase of laser power increases the temperature within the same beam spot, which increases the TE force on the particle. This indicates that the trapping stiffness varies linearly with increasing laser power. An increasing trend is also observed in the experiments, although the trend is not linear at higher powers. This is due to the increase in the Rayleigh−Benard convection that causes destabilization of the particle within the trap. Also, the temperature of the particle within the trap increases, leading to higher Brownian motion. These destabilization effects were not included in the simulation, which leads to an overestimation of the trapping stiffness at the higher laser powers, contradicting the expected linear trend in the system. Conventional optical tweezers do not have such destabilizing effect, thereby obtaining a near-linear trend.[30]

Surfactant Concentration. A change in the concentration of the surfactant alters the ζ-potential and the effective charge of the PS particle. As particle−solvent interfacial characteristics are not well established in the literature, ζ-potential is experimentally evaluated for dispersions of PS particles in varying concentrations of CTAC. The trapping stiffness is measured as a function of concentration of CTAC at a constant laser power of 135 μW. The trapping stiffness increases with the surfactant concentration in the lower regime before saturation is observed. Figure 3b shows an excellent match between theoretical estimates and experimental values. However, at relatively high concentrations (>12 mM), the size of the micelle increases, increasing the vertical depletion forces on the PS particle and thus resulting in suppression of Brownian motion. At such high concentrations, experimental realization of dynamic manipulation of particles is not achievable at low laser powers. Therefore, the experimental value of trapping stiffness is higher than the theoretically expected one. To avoid complications involved with manipulating particles in high CTAC concentration, the concentration of CTAC at the onset of saturation (5 mM in this work) is preferred for maximizing the TE force from the application point of view.

Size Dependence. The trapping stiffness as a function of size of particle is studied to further test the versatility of our theory. As particle size increases, trapping stiffness increases due to an increase in the surface charge of the particle, as shown in Figure 3c. Also, increase in size of the particle leads to a decrease in the diffusion coefficient of the particle, leading to enhanced trapping stiffness. The matching values of the theoretical and measured trapping stiffnesses suggest that the effect of size has already been inscribed within the model during the numerical integration of $E_{T,\|}$ carried over the particle surface. However, correction factors must be included when we deal with smaller particles (<100 nm) to account for surface curvature, thus changing the $\sigma-\zeta$ relationship.[31]

DOI: 10.1021/acs.jpcc.9b06425
J. Phys. Chem. C 2019, 123, 21639−21644

CONCLUSIONS

The modeling technique in this work is based on the decomposition of the TE field around the particle, which can also be extended to model dielectric particles' motion under electrophoresis. For metallic particles, electrons are free to move within the particle under the influence of TE field, and therefore, the effect of perpendicular and parallel components of the TE field varies, compared to dielectric particles. However, this variation is not expected to be very high for nanoparticles in OTET as the dielectric layer of CTAC adsorbed on the particle surface makes the particle behave like a dielectric toward the thermoelectric field.

In summary, we have developed a thermo-electro-mechanical framework to calculate TE forces on dielectric particles under small temperature gradients by incorporating the temperature variation caused by the particle. Although the variations do not alter the bulk TE field much, they must be taken into account in evaluating TE force on the particle, thereby suggesting a role of thermal conductivity of particle in TE field evaluation. A corrective term to include the thermal conductivity contrast was used to estimate the thermodiffusion coefficient and thermophoretic drift of the particle in several works.[1,3,20,32] See Supporting Information Note VII for comparison of thermoelectric forces based on the current work and those using a point particle assumption and correction factor. A good agreement between both the quantities is observed. However, in the previous works, the corrective term was limited to spherical particles and did not consider particles with subparticle thermal conductivity variation, which can easily be implemented in the current work by altering the computational geometry of the particles. The methodology in this work can be further applied to light-absorbing particles, where the temperature gradient arises from the inherent nonuniform optical heating of the particle. We can further incorporate the particle surface characteristics into the model at subparticle resolution, leading to a better TE force and torque estimate for a broader range of particles (e.g., Janus particles and core−shell particles). With recent advances in numerical solvers and visualization techniques, temperature distributions of arbitrarily shaped objects in complex environments can be retrieved to determine TE force accurately, which would lead to the optimum performances of end applications such as thermoelectric trapping and manipulation and provide a new way toward exploring cellular biology.

ASSOCIATED CONTENT

Supporting Information

The Supporting Information is available free of charge on the ACS Publications website at DOI: 10.1021/acs.jpcc.9b06425.

Soret coefficient of micelles; derivation of salinity expression; ζ-potential measurements; experimental setup; sample preparation and trapping; stiffness determination; optical and osmotic force evaluation of particle; comprehensive details of simulation; comparison of thermoelectric forces using numerical integration and corrective terms (Notes I−VII) (PDF)

AUTHOR INFORMATION

Corresponding Authors

*E-mail: linlh2019@mail.tsinghua.edu.cn (L.L.).
*E-mail: zheng@austin.utexas.edu (Y.Z.).

ORCID

Yuebing Zheng: 0000-0002-9168-9477

Author Contributions

P.S.K., L.L., and Y.Z. conceived the idea. P.S.K. performed simulations and experiments. Y.Z. supervised the project.

Notes

The authors declare no competing financial interest.

ACKNOWLEDGMENTS

The authors acknowledge the financial supports of the National Science Foundation (NSF-CMMI-1761743), the Army Research Office (W911NF-17-1-0561), the National Aeronautics and Space Administration Early Career Faculty Award (80NSSC17K0520), and the National Institute of General Medical Sciences of the National Institutes of Health (DP2GM128446). They thank Xiaolei Peng, Yaoran Liu, and Hongru Ding for their intellectual discussions in this work. They also acknowledge the Texas Advanced Computing Center at The University of Texas at Austin (http://www.tacc.utexas.edu) for providing high-performance computing resources that have contributed to the research results reported in this paper.

REFERENCES

(1) Würger, A. Transport in Charged Colloids Driven by Thermoelectricity. *Phys. Rev. Lett.* **2008**, *101*, No. 108302.
(2) Lenglet, J.; Bourdon, A.; Bacri, J. C.; Demouchy, G. Thermodiffusion in Magnetic Colloids Evidenced and Studied by Forced Rayleigh Scattering Experiments. *Phys. Rev. E* **2002**, *65*, No. 031408.
(3) Putnam, S. A.; Cahill, D. G. Transport of Nanoscale Latex Spheres in a Temperature Gradient. *Langmuir* **2005**, *21*, 5317−5323.
(4) Vigolo, D.; Buzzaccaro, S.; Piazza, R. Thermophoresis and Thermoelectricity in Surfactant Solutions. *Langmuir* **2010**, *26*, 7792−7801.
(5) Reichl, M. R.; Braun, D. Thermophoretic Manipulation of Molecules inside Living Cells. *J. Am. Chem. Soc.* **2014**, *136*, 15955−15960.
(6) Lin, L.; Peng, X.; Wei, X.; Mao, Z.; Xie, C.; Zheng, Y. Thermophoretic Tweezers for Low-Power and Versatile Manipulation of Biological Cells. *ACS Nano* **2017**, *11*, 3147−3154.
(7) Lin, L.; Peng, X.; Wang, M.; Scarabelli, L.; Mao, Z.; Liz-Marzán, L. M.; Becker, M. F.; Zheng, Y. Light-Directed Reversible Assembly of Plasmonic Nanoparticles Using Plasmon-Enhanced Thermophoresis. *ACS Nano* **2016**, *10*, 9659−9668.
(8) Lin, L.; Peng, X.; Mao, Z.; Wei, X.; Xie, C.; Zheng, Y. Interfacial-Entropy-Driven Thermophoretic Tweezers. *Lab Chip* **2017**, *17*, 3061−3070.
(9) Vigolo, D.; Rusconi, R.; Stone, H. A.; Piazza, R. Thermophoresis: Microfluidics Characterization and Separation. *Soft Matter* **2010**, *6*, 3489−3493.
(10) Lin, L.; Zhang, J.; Peng, X.; Wu, Z.; Coughlan, A. C. H.; Mao, Z.; Bevan, M. A.; Zheng, Y. Opto-Thermophoretic Assembly of Colloidal Matter. *Sci. Adv.* **2017**, *3*, No. e1700458.
(11) Peng, X.; Lin, L.; Hill, E. H.; Kunal, P.; Humphrey, S. M.; Zheng, Y. Optothermophoretic Manipulation of Colloidal Particles in Nonionic Liquids. *J. Phys. Chem. C* **2018**, *122*, 24226−24234.
(12) Lin, L.; Hill, E. H.; Peng, X.; Zheng, Y. Optothermal Manipulations of Colloidal Particles and Living Cells. *Acc. Chem. Res.* **2018**, *51*, 1465−1474.
(13) Liu, Y.; Lin, L.; Bangalore Rajeeva, B.; Jarrett, J.; Li, X.; Peng, X.; Kollipara, P.; Yao, K.; Akinwande, E.; Dunn, A. K.; et al. Nanoradiator-Mediated Deterministic Opto-Thermoelectric Manipulation. *ACS Nano* **2018**, *12*, 10383−10392.

(14) Braibanti, M.; Vigolo, D.; Piazza, R. Does Thermophoretic Mobility Depend on Particle Size? *Phys. Rev. Lett.* **2008**, *100*, No. 108303.
(15) Piazza, R.; Guarino, A. Soret Effect in Interacting Micellar Solutions. *Phys. Rev. Lett.* **2002**, *88*, No. 208302.
(16) Fayolle, S.; Bickel, T.; Le Boiteux, S.; Würger, A. Thermodiffusion of Charged Micelles. *Phys. Rev. Lett.* **2005**, *95*, No. 208301.
(17) Huang, B. T.; Roger, M.; Bonetti, M.; Salez, T. J.; Wiertel-Gasquet, C.; Dubois, E.; Cabreira Gomes, R.; Demouchy, G.; Mériguet, G.; Peyre, V.; et al. Thermoelectricity and Thermodiffusion in Charged Colloids. *J. Chem. Phys.* **2015**, *143*, No. 054902.
(18) Würger, A. Thermal Non-Equilibrium Transport in Colloids. *Rep. Prog. Phys.* **2010**, *73*, No. 126601.
(19) Sehnem, A. L.; Figueiredo Neto, A. M.; Aquino, R.; Campos, A. F. C.; Tourinho, F. A.; Depeyrot, J. Temperature Dependence of the Soret Coefficient of Ionic Colloids. *Phys. Rev. E* **2015**, *92*, No. 042311.
(20) Piazza, R.; Parola, A. Thermophoresis in Colloidal Suspensions. *J. Phys. Condens. Matter* **2008**, *20*, No. 153102.
(21) Morthomas, J.; Würger, A. Thermoelectric Effect on Charged Colloids in the Hückel Limit. *Eur. Phys. J. E* **2008**, *27*, 425−434.
(22) Majee, A.; Würger, A. Collective Thermoelectrophoresis of Charged Colloids. *Phys. Rev. E* **2011**, *83*, No. 061403.
(23) Lin, L.; Wang, M.; Peng, X.; Lissek, E. N.; Mao, Z.; Scarabelli, L.; Adkins, E.; Coskun, S.; Unalan, H. E.; Korgel, B. A.; et al. Opto-Thermoelectric Nanotweezers. *Nat. Photonics* **2018**, *12*, 195−201.
(24) Agar, J. N.; Mou, C. Y.; Lin, J. L. Single-Ion Heat of Transport in Electrolyte Solutions. A Hydrodynamic Theory. *J. Phys. Chem. A* **1989**, *93*, 2079−2082.
(25) Roelants, E.; De Schryver, F. C. Parameters Affecting Aqueous Micelles of CTAC, TTAC, and DTAC Probed by Fluorescence Quenching. *Langmuir* **1987**, *3*, 209−214.
(26) Brown, M. A.; Abbas, Z.; Kleibert, A.; Green, R. G.; Goel, A.; May, S.; Squires, T. M. Determination of Surface Potential and Electrical Double-Layer Structure at the Aqueous Electrolyte-Nanoparticle Interface. *Phys. Rev. X* **2016**, *6*, No. 011007.
(27) Ly, A.; Majee, A.; Würger, A. Nanoscale Seebeck Effect at Hot Metal Nanostructures. *New J. Phys.* **2018**, *20*, No. 025001.
(28) Cardenas, M.; Schillén, K.; Nylander, T.; Jansson, J.; Lindman, B. DNA Compaction by Cationic Surfactant in Solution and at Polystyrene Particle Solution Interfaces: A Dynamic Light Scattering Study. *Phys. Chem. Chem. Phys.* **2004**, *6*, 1603−1607.
(29) Ohsawa, K.; Murata, M.; Ohshima, H. Zeta Potential and Surface Charge Density of Polystyrene-Latex; Comparison with Synaptic Vesicle and Brush Border Membrane Vesicle. *Colloid Polym. Sci.* **1986**, *264*, 1005−1009.
(30) Rohrbach, A. Stiffness of Optical Traps: Quantitative Agreement between Experiment and Electromagnetic Theory. *Phys. Rev. Lett.* **2005**, *95*, No. 168102.
(31) Doane, T. L.; Chuang, C. H.; Hill, R. J.; Burda, C. Nanoparticle ζ-Potentials. *Acc. Chem. Res.* **2012**, *45*, 317−326.
(32) Piazza, R. "Thermal Forces": Colloids in Temperature Gradients. *J. Phys. Condens. Matter* **2004**, *16*, S4195−S4211.

DOI: 10.1021/acs.jpcc.9b06425
J. Phys. Chem. C 2019, 123, 21639−21644